



Contents lists available at ScienceDirect

## International Journal of Mining Science and Technology

journal homepage: [www.elsevier.com/locate/ijmst](http://www.elsevier.com/locate/ijmst)

# Numerical simulation of gas migration into mining-induced fracture network in the goaf

Cao Jie <sup>a,b,\*</sup>, Li Wenpu <sup>c</sup><sup>a</sup> State Key Laboratory of Gas Disaster Detection, Prevention and Emergency Control, Chongqing 400037, China<sup>b</sup> Chongqing Research Institute Co. Ltd. of China Coal Technology and Engineering Group, Chongqing 400037, China<sup>c</sup> State Key Laboratory of Coal Mine Disaster Dynamics and Control, Chongqing University, Chongqing 400044, China

## ARTICLE INFO

## Article history:

Received 11 December 2016

Received in revised form 17 February 2017

Accepted 17 March 2017

Available online 19 May 2017

## Keywords:

Gas migration

Fractures

Mining-induced

Numerical simulation

## ABSTRACT

Gas extraction practice has been proven for the clear majority of coal mines in China to be unfavorable using drill holes in the coal seam. Rather, mining-induced fractures in the goaf should be utilized for gas extraction. To study gas migration in mining-induced fractures, one mining face of 10th Mine in Pingdingshan Coalmine Group in Henan, China, has been selected as the case study for this work. By establishing the mathematical model of gas migration under the influence of coal seam mining, discrete element software UDEC and Multiphysics software COMSOL are employed to model gas migration in mining-induced fractures above the goaf. The results show that as the working face advances, the goaf overburden gradually forms a mining-induced fracture network in the shape of a trapezoid, the size of which increases with the distance of coal face advance. Compared with gas migration in the overburden matrix, the gas flow in the fracture network due to mining is far greater. The largest mining-induced fracture is located at the upper end of the trapezoidal zone, which results in the largest gas flux in the network. When drilling for gas extraction in a mining-induced fracture field, the gas concentration is reduced in the whole region during the process of gas drainage, and the rate of gas concentration drops faster in the fractured zone. It is shown that with gas drainage, the gas flow velocity in the mining-induced fracture network is faster.

© 2017 Published by Elsevier B.V. on behalf of China University of Mining & Technology. This is an open access article under the CC BY-NC-ND license (<http://creativecommons.org/licenses/by-nc-nd/4.0/>).

## 1. Introduction

The geological conditions of coal seams in China are complex and their permeability is generally low. Gas extraction practice has been proven for the clear majority of coal mines in China to be unfavorable using drill holes in the coal seam. Rather, mining-induced fractures in the goaf should be utilized for gas extraction. In the process of longwall coal mining, the surrounding rock stress is redistributed and generates mining-induced fractures. This is not only favorable for gas desorption off the coal mass, but also it increases the permeability of the coal, thus creating a gas flow channel in the coal and rock mass near the working face. Therefore, research on gas migration into mining-induced fractures above the goaf can provide useful insight, and help optimize the drainage system in terms of pressure-relief and maximize gas extraction rate.

Numerous scholars have carried out research on gas migration laws in mining-induced fracture field above the goaf. Qian and

Xu studied the distribution characteristics of mining-induced fractures in the overlying strata by means of model experiments, image analysis and discrete element simulation [1]. They revealed that a two-stage fracture pattern develops due to mining, in the form of an “O-shape” circle in the long wall face. They also provided a guide to drill hole pattern for relieving gas drainage. Li examined mining-induced fracture field formation and characteristics of fractures above the goaf and in front of the working face [2]. Tu and Liu researched the formation, development, closure and variation of cracks in the roof of the coal seam, and the influence of coal mining. They also described the range of fracture development [3]. Liu et al. according to the breakage and fractures developing in overlying strata, defined the layer area where the fracture aperture was more than  $10^{-1}$  mm as a mining gas channel [4]. Other researchers studied coal seam gas migration laws by numerical simulation, but only a few quantitative results have been reported [5–13]. This is mainly due to the lack of better numerical simulation tools, capable of representing not only the space-time evolution of mining-induced fractures, but also the flow rule of gas migration.

\* Corresponding author at: State Key Laboratory of Gas Disaster Detection, Prevention and Emergency Control, Chongqing 400037, China.

E-mail address: [cqcaoj@126.com](mailto:cqcaoj@126.com) (J. Cao).

This study takes one mining face of 10th Mine in Pingdingshan Coalmine Group in Henan, China as a case study site. Numerical modelling of different gas flow laws in different zones in the working face is carried out by combining multi-physics software COMSOL and discrete element software UDEC. These are used to examine gas migration rule in mining-induced fractures above the goaf.

## 2. Mathematical model for gas migration under the influence of mining

The presence of mining fissures renders the medium porous; the gas in the fissures can be regarded as ideal gas mixture, consisting of methane and air. The gas flow follows the continuity equation, momentum equation and mass conservation equation.

### 2.1. Continuity equation

The gas flow in the coal and rock follows the law of mass conservation. When not considering the mass source (sink), the gas continuity equation is

$$\frac{\partial(\rho_g \phi)}{\partial t} + \nabla \cdot (\rho_g \phi \mathbf{v}_g) = 0 \quad (1)$$

where  $\rho_g$  is the density of the ideal gas, kg/m<sup>3</sup>;  $\phi$  the porosity, %; and  $\mathbf{v}_g$  the flow velocity of gas, m/s. The gas transportation in mining fissure should satisfy the law of conservation of the gas quality, i.e. it should consider the mass sources of gas, so the gas continuity equation is

$$\frac{\partial(\rho_g c_g)}{\partial t} + \frac{\partial}{\partial x_i} (\rho_g c_g u_i) = - \frac{\partial}{\partial x_i} (J_g u_i) + S_g \quad (2)$$

where  $u_i$  is average flow velocity for porous medium in the  $i$  direction;  $S_g$  the additional production rate of gas source term; and  $J_g$  the gas diffusion flux.

### 2.2. Momentum conservation equation

In a given fluid system, the time variation of its momentum is equal to the sum of the external forces acting on it. For porous media, the momentum conservation equation of the  $i$  direction in the inertial (non-acceleration) coordinate system is

$$\frac{\partial(\rho_g u_i)}{\partial t} + \frac{\partial}{\partial x_j} (\rho_g u_i u_j) = \frac{\partial \tau_{ij}}{\partial x_j} - \frac{\partial p}{\partial x_i} + \rho_g g_i + F_i \quad (3)$$

where  $\tau_{ij}$  is the stress tensor;  $\tau_{ij} = \mu_{eff} \left[ \left( \frac{\partial u_i}{\partial x_j} + \frac{\partial u_j}{\partial x_i} \right) - \frac{2}{3} \frac{\partial u_k}{\partial x_k} \delta_{ij} \right]$ ;  $\delta_{ij}$  Kroneker delta;  $\rho_g g_i$  the gravity force on the  $i$  direction;  $F_i$  the external volume force on the  $i$  direction which is including a custom porous media source term.

### 2.3. Equation of motion

Because of the complex gas flow channel in coal and viscous effects, the equation of motion of the gas flow in the porous media of coal and rock need to be described per the conditions of different areas. Per previous research, Navier-Stokes equation is appropriate to describe the fluid flow in the roadway, whereas the Brinkman equation focusing on the fracture zone considers the characteristics of the fluid pressure and movement, which is appropriate to describe the fluid flow in the caving zone [14]. Using the two equations can help build a working face air flow model, as shown in Fig. 1. The velocity and pressure on the interface are consistent in the region where the gas flow is in accordance with Navier-Stokes and Brinkman model. The velocity and pressure distribution

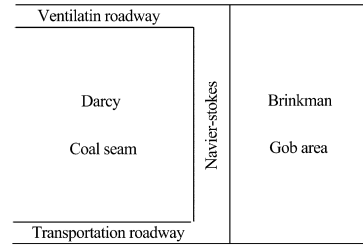


Fig. 1. Schematic plan view showing fluid motion equation in different areas, in front of and behind the working face.

at the coal face and in the goaf can be predicted by the numerical model.

#### 2.3.1. Fluid equation of motion in front of the working face

The Reynolds number,  $Re$  of the gas flow in the coal seam is given by

$$Re = \frac{q \cdot k}{\nu \cdot d_m} \quad (4)$$

where  $q$  is the gas flow velocity, m/s;  $k$  the permeability, m<sup>2</sup>;  $\nu$  coefficient of kinematic viscosity, m<sup>2</sup>/s; and  $d_m$  the average particle size, m. When the  $Re \leq 2320$ , the fluid flow state is laminar flow, it is transition flow when  $2320 < Re < 4000$ , and it is turbulent flow when  $Re \geq 4000$  [15].

When the fluid flow state is laminar, the flow in the coal bed is follows Darcy's Law, which is

$$u = - \frac{k}{\mu} \cdot \frac{dp}{dx} \quad (5)$$

where  $u$  is the gas flow velocity in coal bed, m/s,  $k$  the permeability of coal, m<sup>2</sup>;  $\mu$  the dynamic viscosity of the fluid, Pa/s; and  $dp/dx$  the fluid pressure gradient.

When the fluid flow state is turbulent, the gas flow in the coal bed follows Non-Darcy flow, and the fluid pressure gradient can be expressed as

$$- \frac{dp}{dx} = \frac{\mu}{k} u + \beta \rho u^n \quad (6)$$

where  $n$  is related to the characteristics of the porous media of coal; and  $\beta$  the  $\beta$ -factor of Non-Darcy flow.

Coal permeability in front of the working face is related to its effective stress, considering the dual effect of gas pressure, mechanical effect and absorption effect. The relationship between permeability and effective stress in coal under the condition of mining, i.e. dynamic loading and unloading is

$$k = ck_0 \times \exp \left( d \left\{ \Theta - 3p \left\{ 1 - \frac{3K(1-2\nu_s)}{E_s} \left[ 1 - \frac{\rho RT \alpha \ln(1+bp)}{p(1-\phi)} \right] \right\} \right\} \right) \quad (7)$$

where  $k_0$  is the original permeability of coal, m<sup>2</sup>;  $\Theta$  the bulk stress of coal, MPa;  $K$  the bulk modulus, MPa;  $\nu_s$  the Poisson's ratio of the coal skeleton;  $p$  the gas pressure, MPa;  $\rho$  the density of coal, kg/m<sup>3</sup>;  $a, b$  the isothermal adsorption constants;  $R$  the molar gas constant;  $R = 8.3143$  J/(mol K); and  $\phi$  the porosity, %.

#### 2.3.2. Fluid motion equation in working face

Navier-Stokes equation can well describe the fluid flow in the pipeline, the fluid flow is faster in working face, and it can be solved by Navier-Stokes equation.

$$-\nabla \cdot \eta [\nabla u_{ns} + (\nabla u_{ns})^T] - \rho_g (u_{ns} \cdot \nabla) u_{ns} + \nabla p_{ns} = 0 \quad (8)$$

**Table 1**  
Physical and mechanical parameters of coal and rock strata.

Lithology	Density (kg/cm <sup>3</sup> )	Elasticity modulus (GPa)	Uniaxial compressive strength (MPa)
Mudstone	2.4	17	39.0
Coal	1.4	13	21.0
Sandstone	2.8	41	68.5
Sandy mudstone	2.5	20	42.4
Medium-coarse sandstone	3.1	43	70.6
Fine sandstone	2.6	37	58.2

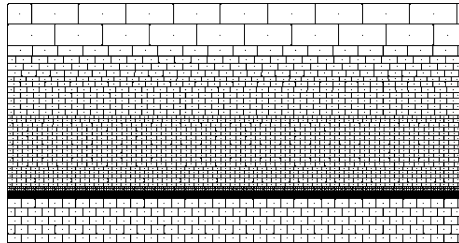


**Fig. 2.** Numerical simulation model.

**Table 2**  
Mechanical properties of joints used in the numerical model.

Lithology	Normal stiffness (GPa)	Shear stiffness (GPa)	Frictional angle (°)
Mudstone	7	1	30
Coal	3	0.3	28
Sandstone	21	15	39
Sandy mudstone	14	7	34
Medium-coarse sandstone	25	17	41
Fine sandstone	19	13	37

$$\nabla \cdot u_{ns} = 0$$

where  $\eta$  is the coefficient of viscosity, kg/(m·s);  $u$  the velocity vector, m/s;  $\rho_g$  the fluid density, kg/m<sup>3</sup>; and  $p$  pressure, MPa. The subscript *ns* means described by the Navier-Stokes equation.

**2.3.3. Fluid equation of motion in the gob area**

The Brinkman equation describes a flow condition between Darcy and Navier-Stokes. The fluid flow in porous media can be described by Darcy’s law when the velocity is small, which does not consider the energy transfer caused by shear stress. When the flow velocity is relatively large, the energy transfer caused by shear stress is considered, and the Brinkman equation is used. This is:

$$-\nabla \cdot \eta[\nabla u_{br} + (\nabla u_{br})^T] - \left(\frac{\eta}{k} u_{br} + \nabla p_{br} - F\right) = 0 \tag{9}$$

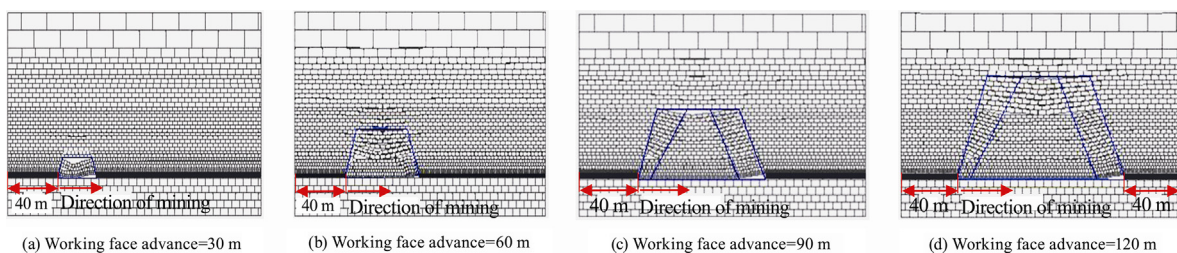


**Fig. 3.** Distribution of mining-induced fracture as the coal working face advances.

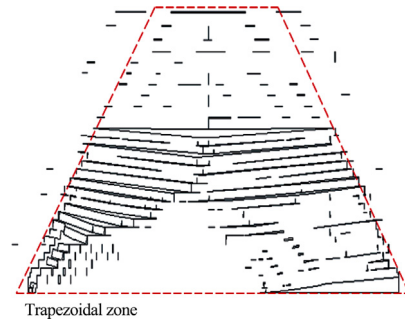


**Fig. 4.** Mining-induced fracture network.

$$\nabla \cdot u_{br} = 0$$

where the subscript *br* denotes the Brinkman equation.

**3. Numerical simulation of overlying strata movement law in mining-induced fractures field**

The fracture field is formed within a certain distance in the overlying strata above the gob area after coal mining. There are two main types: bed-separated fissures and vertical rupture fissures. Overlying strata will incur different degrees of deformation, resulting in different gas migration and accumulation rules depending on the mining-induced fracture field. Therefore, the simulation of overlying strata movement in mining-induced fractures field is first carried out with UDEC software.

**3.1. Numerical model setup**

In this study, the overlying strata movement law in working face 24,080 of 10th Mine of Pingdingshan Tianan Coal Mining Co. Ltd is simulated. The physical and mechanical parameters of coal seam and rock strata are shown in Table 1. As shown in Fig. 2, the model is 200 m × 100 m. The total working face advance distance is 120 m, leaving 40 m of unmined coal on the left and right sides of the model boundaries in order to eliminate the boundary effects. The working face advance is divided into 12 steps of 10 m. The coal seam mining depth simulated is 890 m. The thickness of the coal seam is 2.4 m, the upper model boundary is loaded with 20 MPa, and the left or right side and the bottom of the model are constrained from lateral displacement. The bottom boundary is constrained from vertical displacement. For the simulation of fractures, the mechanical parameters of the joints listed in Table 2 are used.

**3.2. Numerical results**

The evolution raw of the fracture field when the excavation distance is 30, 60, 90, 120 m, as shown in Fig. 3. It can be seen from Fig. 3 that the overlying strata movement is a dynamic spatiotemporal

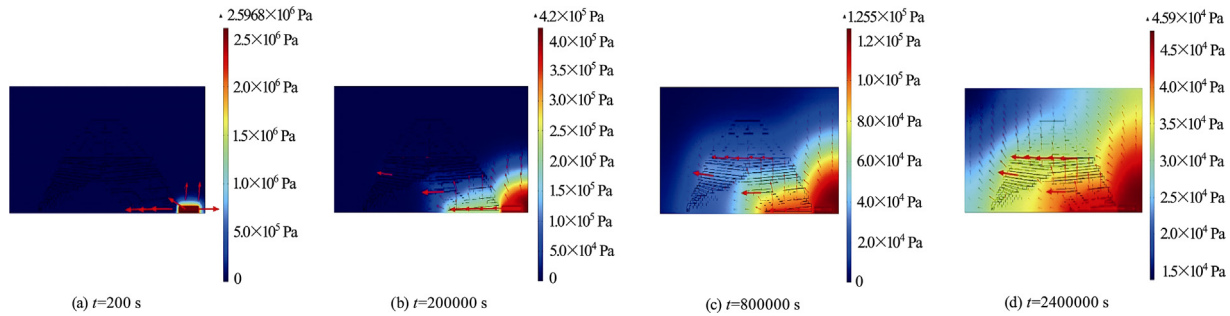


Fig. 5. Simulated gas migration in the mining-induced fracture network at different times using COMSOL.

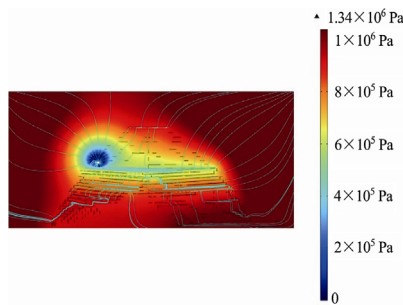


Fig. 6. Gas pressure nephogram and streamline contours of gas flux.

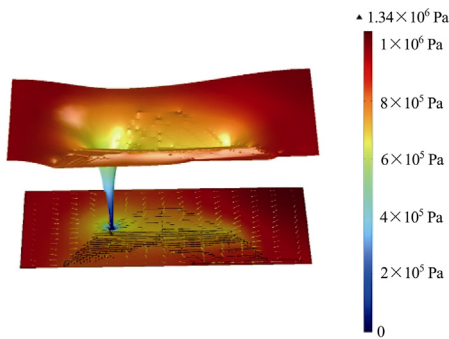


Fig. 7. Gas pressure by height expression.

evolution process. When the working face is advanced to different distances, the overlying strata above the gob forms mining-induced fracture in the shape of a trapezoid. With the increase of the working face advance, the height of the trapezoidal zone also increases.

#### 4. Numerical simulation of gas migration in mining-induced fracture network

The network of mining-induced fractures obtained by UDEC numerical simulation model is shown in Fig. 4. The fracture geometry is then extracted using CORE DRAW software.

The extracted fracture network geometry is then imported into the COMSOL multi-physics software for the numerical simulation, the gas migration at different times in the mining-induced fracture network can be obtained, as shown in Fig. 5. In the initial time ( $t = 0$ ), the initial gas pressure is 3 MPa in coal seam, and is 0.1 MPa in fracture network. The initial velocity is 0. There is no flux around the model. As the time passes, the gas gradually migrates to the fracture network. The size of the arrow in Fig. 5

represents the size of the gas flux. As can be seen from Fig. 5, the gas flux in the mining-induced fracture network is far greater than that in the matrix of overlying strata. The bed-separated fissures and vertical rupture fissures serve as channels for gas flow, compared to the matrix of overlying strata, where the gas flow is limited. As the gas migrates into the mining-induced fracture network, the gas fluxes are larger in the overlying area where the bed separation degree is large. The largest mining-induced fracture is found at the upper end of the trapezoidal zone, which results in the largest gas flux in the network.

Fig. 6 displays gas pressure nephogram and streamline gas flux. Assuming gas flow to a certain time, the gas pressure in the whole region reaches equilibrium, and the gas drainage is carried out in the fractured zone. From the distribution of gas pressure in Fig. 6, it can be seen that gas pressure in the whole region is falling, and the decrease rate is relatively large in the fracture development area.

Fig. 7 shows gas pressure by height expression. As can be seen from Fig. 7, the height in the surrounding coal matrix decreases gradually, then it decreases rapidly in fractured zone of mining-induced field. This implies that gas pressure decrease rate in overlying strata matrix is smaller than that in the fractured zone. It also means that with drainage, gas flow in the mining-induced fracture network is stronger.

#### 5. Conclusions

The mathematical model of gas migration in coal seam is established according to the flow type in different positions. Based on this, using discrete element software UDEC software and multi-physics software COMSOL, the numerical simulation of gas migration into mining-induced fracture network above the goaf is carried out. The UDEC simulation of working coal face advance shows that with the increase of the working coal face distance, a trapezoidal fracture network zone develops; and the height of such zone gradually increases with coal face advance. Using COMSOL, the fracture network is simulated. It is shown that compared with the matrix of overlying strata, the gas flow in fracture zone is more significant. The largest mining-induced fracture is found at the upper end of the trapezoidal zone, which results in the largest gas flux in the network. If gas drainage carried out in the fractured zone, gas concentration decrease rate in overlying strata matrix is smaller than that in the fractured zone. This implies that gas concentration decrease rate in overlying strata matrix is smaller than that in the fractured zone. It also means that with drainage, gas flow in the mining-induced fracture network is stronger.

The analysis presented in this paper is yet to be validated with gas content tests in the field. These will be carried out and reported in future to validate the numerical simulation technique and results presented in this paper.

## Acknowledgments

This study was financially supported by the National Key Research and Development Program (No. 2016YFC0801402), the National Natural Science Foundation of China (No. 51374236), Chongqing Research Program of Basic Research and Frontier Technology of China (No. cstc2015jcyjBX0076).

## References

- [1] Qian MG, Xu JL. Study on the "O-shape" circle distribution characteristics of mining-induced fractures in the overlying strata. *J China Coal Soc* 1998;23(5):466–9.
- [2] Li SG. Gas delivery feature and its control influenced by movement of the surrounding rock in fully-mechanized top coal caving. Xi'an, China: Xi'an University of Science and Technology; 1998.
- [3] Tu M, Liu ZG. Research and application of crack development in mining seam roof. *Coal Sci Technol* 2002;30(7):54–6.
- [4] Liu HY, Cheng YP, Chen HD, Kong SL, Xu C. Characteristics of mining gas channel and gas flow properties of overlying stratum in high intensity mining. *J China Coal Soc* 2012;37(9):1437–43.
- [5] Gao JL. Simulation study on the influence of permeability on gas migration in gob. *China Safety Sci J* 2010;20(9):9–14.
- [6] Liang D, Zhou XH. Numeric simulation on gas movement law in working face. *J Liaon Techn Univ (Natural Sci)* 1999;18(4):337–40.
- [7] Whittles DN, Lowndes IS, Kingman SW, Yates C, Jobling S. Influence of geotechnical factors on gas flow experienced in a UK longwall coal mine panel. *Int J Rock Mech Min Sci* 2006;43(3):369–87.
- [8] Guo H, Yuan L, Shen BT, Qu QD, Xue JH. Mining-induced strata stress changes, fractures and gas flow dynamics in multi-seam long wall mining. *Int J Rock Mech Min Sci* 2012;54:129–39.
- [9] Guo H, Yuan L. An integrated approach to study of strata behaviour and gas flow dynamics and its application. *Int J Coal Sci Technol* 2015;2(1):12–21.
- [10] Guo ZL. Lattice Boltzmann model for incompressible flows through porous media. *Am Phys Soc* 2002;66(3):1–9.
- [11] Teng G, Tan YL, Gao M. Simulation of gas seepage in fissured coal based on lattice Boltzmann method. *Chin J Rock Mechan Eng* 2007;26(supp 1):3503–8.
- [12] Yang MD, Li YM, Zhang H. Numerical simulation of gas concentration field in the partial W-type ventilation system. *J Safety Environ* 2013;13(6):186–90.
- [13] Zhou HW, Liu JF, Xue DJ, Yi HY, Xue JH. Numerical simulation of gas flow process in mining-induced crack network. *Int J Min Sci Technol* 2012;22(6):793–9.
- [14] Yang TH, Chen SK, Zhu WC, Liu HL, Huo ZG, Jiang WZ. Coupled model of gas-solid in coal seams based on dynamic process of pressure relief and gas drainage. *Rock Soil Mech* 2010;31(7):2247–52.
- [15] Xu XL, Wang KS, Meng LM. Fluid mechanics. Beijing: National Defence Industry Press; 2011.